JOURNAL OF PROPULSION AND POWER
Vol. 22, No. 2, March–April 2006

Pressure Distribution on an Eccentric Annular Seal at Fractional Whirl Ratios

A. Suryanarayanan* and G. L. Morrison†
Texas A&M University, College Station, Texas 77840

This paper presents the results of an experimental investigation aimed at understanding the variation of wall pressure distributions for a 50% eccentric annular seal as the whirl ratio is altered from 0 to 1 in incremental steps of 0.1. The test apparatus is constructed such that the stator can be set at different eccentricities and precessed in a circular orbit at a speed set independently of the rotor speed allowing for the fractional whirl ratios. The rotor is mounted concentric on the shaft and operated at a fixed speed of 1800 rpm ($Ta = 3300$) while the stator is mounted eccentrically. Ensemble-averaged transient and mean wall-pressure distributions are measured along the seal axis for a Reynolds number of 2.4×10^4 using water as the working fluid. The results indicate that the peak low and high pressures at the seal exit migrate from the suction zone to the pressure zone between whirl ratios of 0.8 and 0.9. Also the magnitude of pressures measured for the smaller whirl ratios (0.1 to 0.5) are considerably lower than those encountered at the higher whirl ratios (0.6 to 1).

Nomenclature

c	=	nominal clearance between rotor and stator, 1.27 mm
D	=	rotor diameter, 164.1 mm
e	=	rotor eccentricity ratio, 0.5
L	=	rotor length, 35.56 mm
P	=	pressure, kPa
P_{mean}	=	time-averaged pressure
P^*	=	nondimensional pressure, $PL/c\Delta P$
P^*_{mean}	=	nondimensional mean pressure, $(P_{\text{mean}} - P_{Z/L=1.00})/\Delta P$, kPa
Q	=	volumetric flow rate, m^3/s
Re	=	Reynolds number, $= 2\rho U_m c/\mu$
Sn	=	Sommerfeld number, $= 12\pi e/[(1-e^2)^{1/2}(2+e^2)]$
Ta	=	Taylor number, $= (\rho W_{\text{sh}} c/\mu)(2c/D)^{1/2}$
U_m	=	average mean axial velocity, $Q/\pi Dc$, m/s
W_{sh}	=	rotor surface velocity, m/s
Z	=	axial location along the seal, mm
Z/L	=	nondimensionalized axial location along the seal
ΔP	=	pressure drop from seal entrance to exit (Pin-Pout), kPa
μ	=	absolute viscosity, 7.84×10^{-4} kg/m-s
ν	=	kinematic viscosity, μ/ρ, m^2/s
ρ	=	density, 999 kg/m^3
ω	=	whirl ratio, defined as the ratio of the stator rotation rate to the shaft rotation rate
$\langle\,\rangle$	=	phase-averaged quantity

Introduction

SEALS play a vital role in determining the stability and efficiencies of rotating machinery. The effective separation the seals can offer between the high- and low-pressure zones depends on their geometry and the operating conditions. The physical features of the seal-rotor annulus influence the flow through it and consequently the forces on the rotor.[1] The forces generated by seals can be stabilizing or destabilizing depending on the rate at which a shaft orbits (whirls) within the stator. Winslow[2] determined that the radial forces on the rotor caused by the azimuthal shear stresses were two to three orders of magnitude lower than the forces created by the pressure forces. Hence, to obtain a close approximation of the forces created by the flow through the clearance volume, information about the pressure distribution on the seal walls is deemed sufficient. Winslow,[2] Morrison and Winslow,[3] and Robic[4,5] observed that the pressure distribution inside an annular seal changed significantly between a statically eccentric (whirl ratio = 0) and a synchronous whirl condition (whirl ratio = 1). The static case is similar to a jounal bearing, but the region of high and low pressures flipped between the inlet and exit of the seal when it was whirling at the shaft rotation speed. Thus, a continually changing geometry, as in a whirling seal, necessitates the study of the flow in the clearance volume to quantify the pressure distribution and, thus how the forces on the seal vary with whirl ratio.

Kaneko[6] analyzed annular seals for static and dynamic characteristics in the turbulent and laminar regions based on a mixing length theory. He employed the general Reynolds equation for the laminar region and two-dimensional turbulent equations for the transient zone, verifying his results experimentally. The consequences of whirl on rotordynamic coefficients were not considered in this analysis. He also showed that the pressure drop distribution along the seal near the inlet influenced the seal load-carrying capacity as well as the stiffness of the seal. Hashimoto et al.[7] studied the effects of fluid inertia forces on the dynamic characteristics of short journal bearings. He predicted the whirl onset velocities using three lubrication theories, and also examined the shaft speeds for which the system became unstable.

Characterization of the flow inside the seal clearance volume is complicated and cumbersome because of the problems involved with the measurement of flow in small sections. Velocity and turbulence measurements for eccentric annular and labyrinth seals for different Reynolds and Taylor numbers were performed by Johnson,[8] Thames,[9] Das,[10] Shresta,[11] and Morrison et al.[12] using a three-dimensional laser-Doppler-anemometry (LDA) system. They observed how the region of maximum axial velocity remained on the suction side of the seal for a statically eccentric seal but migrated to the pressure side at the seal exit for a synchronous whirl case. This is consistent with the pressure fields observed by Winslow[2] and Robic.[4,5] Arghir and Frene[13,14] theoretically investigated a 50% eccentric smooth annular seal for a whirl ratio of one. The experimental data from Morrison et al.[12] compared well with the results of their analysis. A perturbation technique with averaged Navier–Stokes equations was applied for the investigation to account for the eccentricity and also the synchronous whirl conditions.

Presented as Paper 2003-4832 at the AIAA/ASME/SAE/ASEE 39th Joint Propulsion Conference, Huntsville, AL, 20–23 July 2003; received 10 August 2004; revision received 28 April 2005; accepted for publication 2 May 2005. Copyright © 2005 by the American Institute of Aeronautics and Astronautics, Inc. All rights reserved. Copies of this paper may be made for personal or internal use, on condition that the copier pay the $10.00 per-copy fee to the Copyright Clearance Center, Inc., 222 Rosewood Drive, Danvers, MA 01923; include the code 0748-4658/06 $10.00 in correspondence with the CCC.

*Graduate Student, Mechanical Engineering Department.
†Nelson-Jackson Professor, Mechanical Engineering Department. Associate Fellow AIAA.

The instantaneous and phase-averaged wall pressures for annular and labyrinth seals with dynamic eccentricities and a whirl ratio of one were recorded by Winslow[2] and for different preswirls by Robic[4,5] at $Re = 2.4 \times 10^4$ and $Ta = 3300$. The data they collected showed that the peak positive and suction pressures switched positions at the seal exit between a nonwhirling and a whirling case for the same eccentricity. This implied that the pressure forces also changed locations as the whirl ratio varied between 0 to 1 reaching a minimum at an intermediate whirl before increasing on the opposite side of the seal.

In short, all of the investigations listed deal mainly with the study of either concentric, statically eccentric, or synchronously whirling seals with very little information for clearance flows in a fractionally whirling seal. Hence, to study the effects of fractional whirls on the clearance flow and also to ascertain the circumstances under which the peak pressures changed locations, the current work endeavors to measure the mean and dynamic wall-pressure distributions on a smooth annular seal for the following test conditions: 1) eccentricity is 50% of the seal-stator clearance, 2) $Re = 2.4 \times 10^4$, 3) rotor speed is $Ta = 3300$ (1800 rpm), 4) whirl ratio is 0 to 1 for rotor speed of 1800 rpm, and 5) zero forced preswirl.

The test parameters were chosen in keeping with the previous experiments conducted by Morrison[3] and Morrison et al.[12,15,16]

The pressure distributions obtained for the different whirl ratios can be integrated along the seal circumference to determine the forces and the moments generated by the differential flow in the clearance volume.[4] Knowing the pressure distribution along the seal wall for different whirl ratios can possibly assist in determining the appropriate conditions under which the rotor experiences minimal stress and the same can be used to operate the system. Further, the pressure information can form the basis for the calculation of rotordynamic coefficients for fractionally whirling seals. Based on the obtained stiffness and damping coefficients, the geometry of the seal can be modified to suit specific requirements, thus leading to a better design. Because few data exist for annular seals at fractional whirls, the information from the study can be used for future simulation work.

Experimental Facility

The test facility used for this work can be broadly classified into four distinct units: 1) the water supply system, 2) the seal test facility, 3) eccentricity and whirl setting unit, and 4) instrumentation.

Water to the test facility is supplied from a 19-m^3 tank by a centrifugal pump driven by a 29.5-kW motor. The water temperature in the test facility is maintained at 30.5 ± 4°C using a 70-kW heat exchanger in order to maintain the thermal expansion of the seal within limits. The water entering the test section is cleaned of all floating debris by a 10-μ filter located at the pump exit and a wire mesh just ahead of the seal.

The test section is composed of a rotor-stator seal arrangement (Fig. 1) in which the rotor is mounted on an overhung shaft of diameter 50.8-mm run by a 37-kW variable speed motor capable of speeds up to 5300 rpm. The rotor, which also serves as a seal, is enclosed in a stainless-steel stator of inner diameter 166.64 mm. The rotor-stator clearance measures 1.27 rhm on the radius. The seal is made of acrylic, which has the following mechanical properties[8]: Young's modulus, 1.24×10^{10} Pa; density, 913 kg/m^3; ultimate strength, 9.507×10^{10} Pa; and coefficient of thermal expansion, 41×10^{-6} mm/°C.

Das[10] used a "hoop stress analysis for a thin cylindrical body" method to analyze the mechanical growth of the seal. He reckoned that the seal expanded by 0.0386 mm (3% of the clearance), at a rotor speed of 3600 rpm and by 0.006 mm/°C (0.4% of the clearance for the 8°C test temperature window) with changes in temperature. Bending of the rotor for maximum tip loading was measured by Robic.[4] The maximum deflection measured at the rotor extremity for a load of 88.96 N (20 lbf) was 0.04 mm (1.6 mils) or 3.2% of the clearance. Thus the variation of clearance during the operation of the facility under extreme loading was calculated to be a maximum of 6.6% of the clearance. This implies that under adverse conditions the clearance will have a maximum variation of 6.6% in addition to the 50% eccentricity already being set.

The conceptualized design for the eccentricity and whirl setting unit is an inexpensive and reliable method to obtain the required fractional whirl ratios for different eccentricities. The test facility is redesigned to oscillate the stator independently of the rotor to simulate the whirl ratios. Variable whirl ratios are obtained by oscillating the stator independent of the rotor by way of the cam system shown in the Fig. 2. Two independent cam-operated plunger units shown in Fig. 2 oscillate the stator at varying frequencies and amplitudes. The plungers are located orthogonal to each other on the stator and affect the vertical and the horizontal oscillations of the stator as well as making it whirl when working in unison. The phase between the two plunger units is set by changing the length of the timing belt driving the system using an idler pulley positioned between the two plunger shafts. The phase fixed between the two plungers determines the orbital path of the stator. The required eccentricities can be set by adjusting the eccentricity of the cams. For the static or zero whirl case (which is similar to a statically eccentric journal bearing condition), a circular graded scale similar to a protractor was designed and mounted concentric to the whirl motor pulley. The eccentric stator was held at a known angle, and pressure measurements were acquired through 0 to 360 deg. Figure 3 shows the eccentric whirling of the rotor with respect to the stator and also graphically depicts a stator cycle.

The instrumentation consists of pressure transducers, the associated signal conditioners, and the data-acquisition system. The mean pressure distribution at 17 axial locations along the seal length is measured using a Validyne pressure transducer connected to a Scani-Valve. The accuracy of the data output from the system is 1.5% of the measured value. Piezoresistive Kulite pressure transducers having a rated sensitivity of 0.35 mV/kPa (2.5 mV/psi) and a frequency response of 120 kHz were used to measure the instantaneous pressures

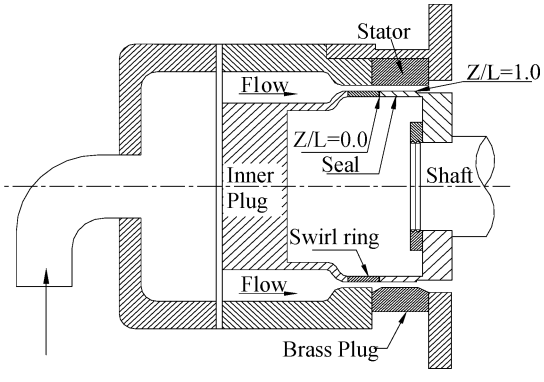

Fig. 1 Cross-sectional view of the seal test rig.

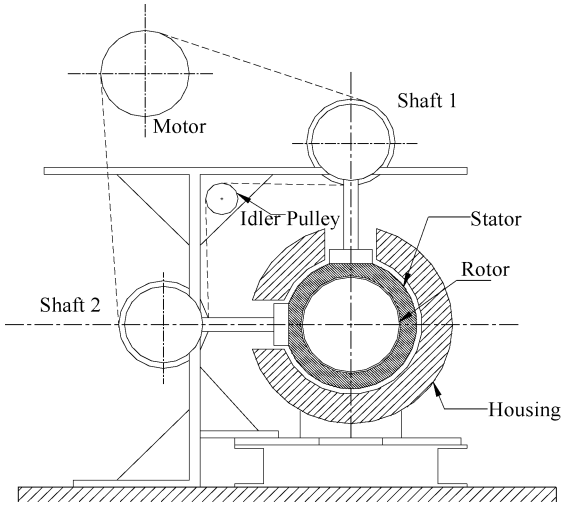

Fig. 2 Basic sketch of the test rig with whirl setup.

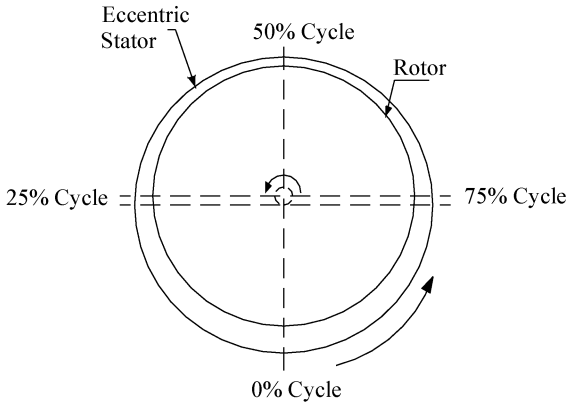

Fig. 3 Cyclic representation of whirl.

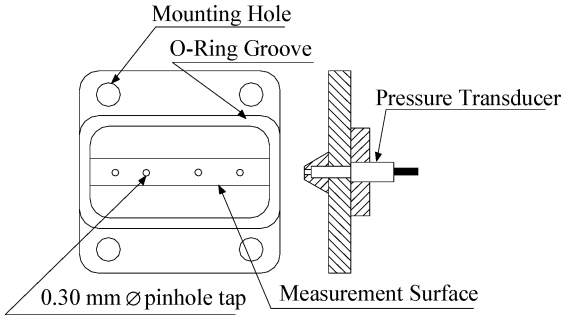

Fig. 4 Piezoresistive pressure transducer mounting brass block.

in accordance with the recommendations of Olivero-Bally et al.[17] and Nunes.[18] Four brass plugs (Fig. 4) with 0.3-mm Ø pinholes at different axial locations were manufactured to hold the Kulite transducers flush with the stator inner wall. The 0.3-mm Ø pinholes provided high spatial resolution of the pressure field. Olivero-Bally et al.[17] measured the wall-pressure fluctuations in turbulent boundary layers and determined that flush-mounted pinhole piezoresistive pressure transducers were appropriate for acquiring data in the high frequency or turbulent region of flow. The transducers were exposed to the flow through 0.3-mm holes to minimize spatial averaging effects. Nunes[18] performed a comparison between a ScaniValve system and piezoresistive transducers for measuring dynamic wall pressure and found the piezoresistive transducers to work better in the transient pressure zones. The trigger for ensemble averaging the instantaneous pressure data was provided by an optical probe sensing the whirl shaft key way. The orbital of the stator was monitored using two orthogonally positioned proximity probes.

Experimental Results

The annular seal was tested at $Re = 2.4 \times 10^4$ corresponding to a flow rate of 4.86 ± 0.05 l/s and a rotor speed of 1800 rpm ($Ta = 3300$). The axial positions Z along the seal were normalized using the seal length L, $Z/L = 0$ corresponding to the seal entrance and $Z/L = 1$ the exit. The axial mean pressure along the stator length is normalized by the seal inlet and the outlet pressures.

$$P^*_{\text{mean}} = (P_{\text{mean}} - P_{\text{out}})/(P_{\text{in}} - P_{\text{out}})$$

Similarly the axial phase-averaged dynamic pressure was normalized using the seal length L, mean pressure drop ΔP across the seal, and the seal clearance c, when the rotor is centered. The equation used is as follows:

$$\langle P^* \rangle = \langle P \rangle L/c\Delta P$$

Variation of Normalized Mean Pressure P^*_{mean} and Pressure Drop ΔP Across the Seal Inlet and Exit with Changes in Whirl Ratio

The general mean pressure distribution for all of the positive whirl ratios shown in Fig. 5 follow the trend observed by Robic[4] and Winslow.[2] The normalized mean pressure distribution experiences a small increase near the inlet region. This is followed by a rapid drop in pressure as the flow enters the small clearance annulus. Flow measurements by Morrison et al.[12] have shown that there exists a flow separation on the rotor surface just inside the seal. The slight pressure recovery seen at $Z/L = 0.35$ is caused by the flow reattaching to the rotor. Downstream of $Z/L = 0.4$, the pressure decreases in an almost linear fashion acted upon by only the wall frictional forces. The influence of the downstream diverging section on the flow at the exit is not discernible as the mean pressure continues to decrease. The pressure increase observed near the seal entrance is primarily caused by effects of the seal inlet geometry. The inner plug generates a diverging section just upstream of the seal inlet. This is present to increase the swirl angle when upstream swirl generators are installed. The entering flow also faces a varying step as the stator orbits around the seal. The entrance constriction encountered by the flow caused by the rotor eccentricity also affects the flow up to an axial position of $Z/L = 0.1$–0.15 before the flow recovers.

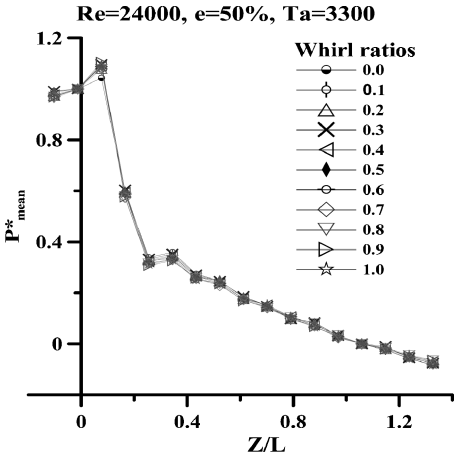

Fig. 5 Effect of ω on normalized mean pressure.

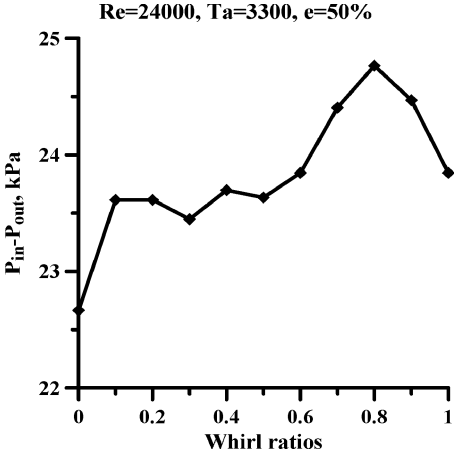

Fig. 6 Effect of ω on ΔP across the seal inlet and exit.

The normalized axial mean pressure distributions for all of the whirls coincide with each other indicating that the mean axial pressure distribution is independent of rotor fractional whirls. This is consistent with the findings of Robic,[4] who noted that the ratio of $dP^*_{\text{mean}}/dZ/L$ was mainly dependent upon the Reynolds and Taylor number and not on the rotor whirl. Figure 6 represents the overall pressure drop across the seal for whirl ratios between 0.0 and 1. The general trend shows a sudden increase of 5% as the seal begins to whirl. From 0.1 to 0.5, the pressure drop is relatively constant. It increases another 5% as the whirl ratio increases from 0.5 to 0.8. This is followed by a decrease of 5% from 0.8 to 1 whirl ratio. Even though the normalized mean pressure axial distribution is invariant with whirl ratio, the absolute value of the pressure drop across the

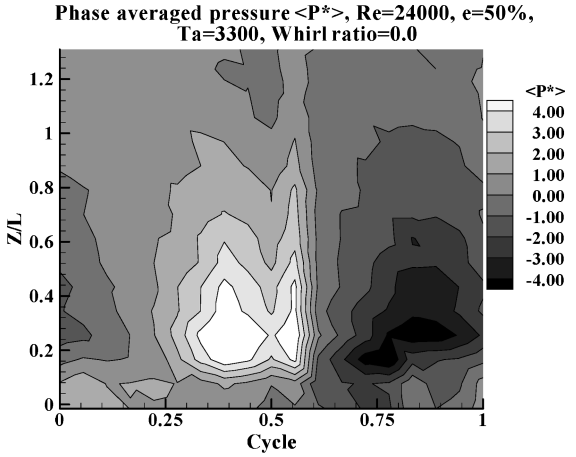

Fig. 7 Phase-averaged pressure contours, whirl ratio = 0.0.

seal varies 10% for a constant leakage rate. The phase-averaged instantaneous pressures will be analyzed next to help determine the cause.

Variation of Phase-Averaged Instantaneous Pressure $\langle P^* \rangle$ with Changes in Whirl Ratios

The phase-averaged experimental results for the cases tested are discussed in the following section. The rotor spins in the counterclockwise direction when viewed from the front of the test facility. Positive whirl ratios are obtained by spinning the stator in the same direction as the rotor. Each cycle is considered with respect to one complete stator rotation. Figure 7 presents data for the no-whirl condition. This is essentially a short journal bearing with axial flow imposed upon it. The cycle begins with the maximum clearance location (0%), followed by the pressure side of the seal (0–50%) where the clearance is decreasing, the minimum clearance occurring at 50% of the stator cycle, and then the suction side of the seal (50–100%), where the clearance is increasing. The pressure distribution at the seal entrance is very similar to a journal bearing. The pressure gradually increases over the first 20% of the seal circumference, then increases rapidly to a maximum near the minimum clearance. Because of the small but finite amount of preswirl generated by the seal upstream of the seal entrance, the location of maximum pressure persists past the minimum clearance and decreases gradually to the low-pressure values on the suction side of the rotor at about 75% of the cycle. The pressure then begins to increase after 90% of the seal circumference. The pressure distribution over the first 35% of the seal length is very similar to a statically eccentric journal bearing except for the high- and low-pressure locations being offset toward the suction side of the seal. This effect is in the same direction as the flow preswirl. The axial flow through the seal destroys the journal-bearing-type pressure distribution as the flow progresses through the seal with almost no azimuthal variation remaining at the seal exit.

The infinitely long Sommerfeld journal bearing analysis was applied using the geometry and operating conditions of this seal to compare predictions with the pressure magnitudes measured in the seal. The nondimensional Sommerfeld number has a value of 9.7 with a maximum pressure prediction of 2.8 in the nondimensional format used in Fig. 7. This is lower than the measured value of 7. There are several possibilities for the differences. The leakage flow and the finite length of the seal compared to the infinite length and zero axial-velocity component in the theory will surely affect the results. There is also a preswirl present in the experimental work, which shifts the pressure distribution in the direction of rotation. However, the largest effect is most likely the flow separation inside the seal entrance observed by Morrison et al.[15] A 20% reduction of the seal clearance produces a journal bearing maximum pressure of 8.4, very similar to the measurements. This is a turbulent flowfield, whereas the Sommerfeld analysis is for laminar flow. Yet, the close agreement is quite enlightening.

The phase-averaged dynamic pressure distributions for a rotor speed of 1800 rpm ($Ta = 3300$) and positive whirl ratios between 0.1 and 1 are shown in Figs. 8–17. The addition of whirl to a value of 0.1 greatly disrupts the journal-bearing-type pressure field by decreasing the amplitude of the pressure variance and suppressing the steep azimuthal pressure gradient at the minimum clearance location near the seal inlet. The azimuthal location of maximum and minimum pressure remains about the same for the 0 and 0.1 whirl ratio cases. The major difference between the two cases is

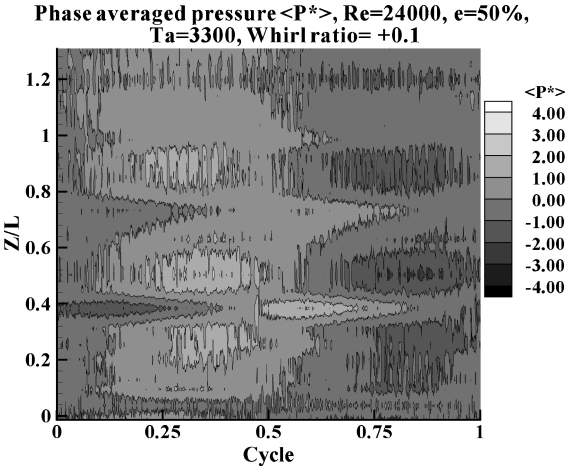

Fig. 8 Phase-averaged pressure contours, whirl ratio = 0.1.

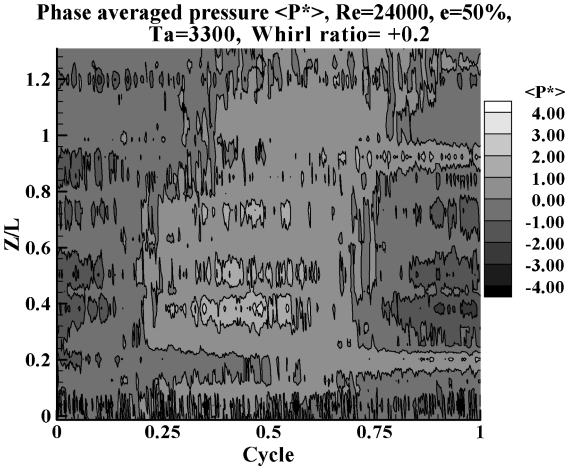

Fig. 9 Phase-averaged pressure contours, whirl ratio = 0.2.

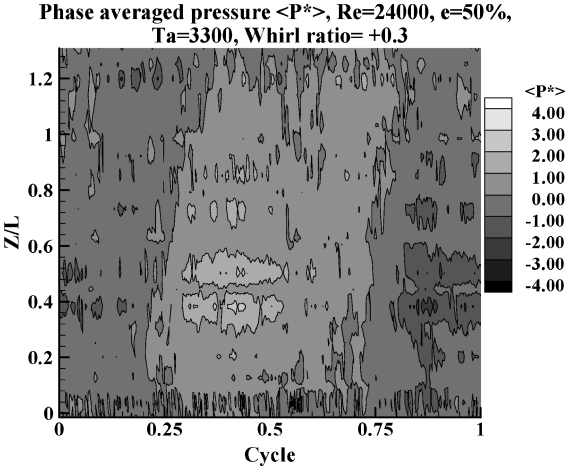

Fig. 10 Phase-averaged pressure contours, whirl ratio = 0.3.

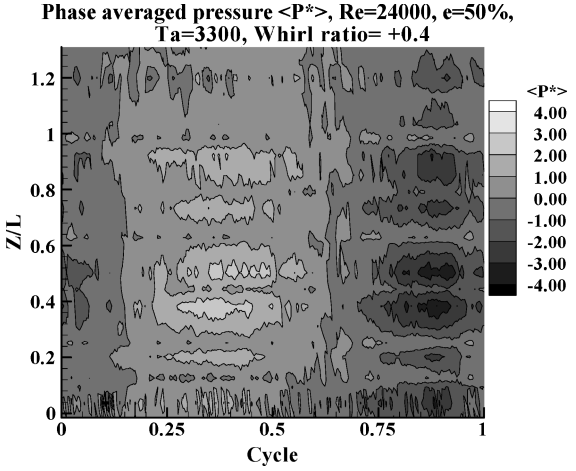

Fig. 11 Phase-averaged pressure contours, whirl ratio = 0.4.

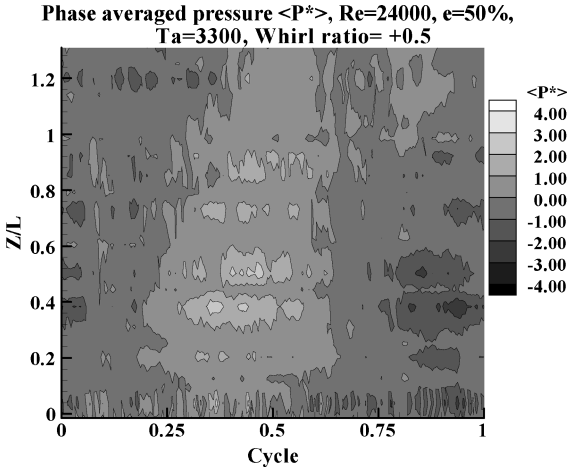

Fig. 12 Phase-averaged pressure contours, whirl ratio = 0.5.

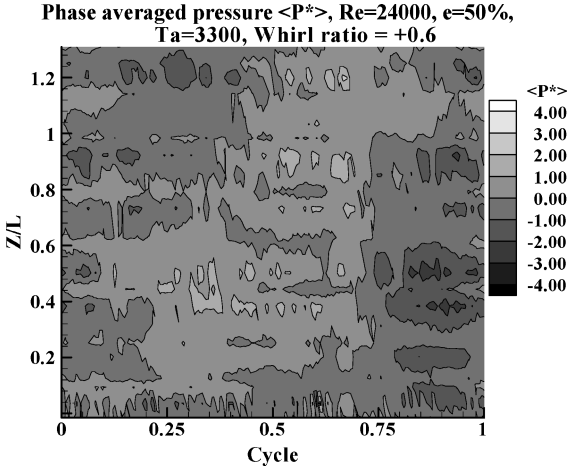

Fig. 13 Phase-averaged pressure contours, whirl ratio = 0.6.

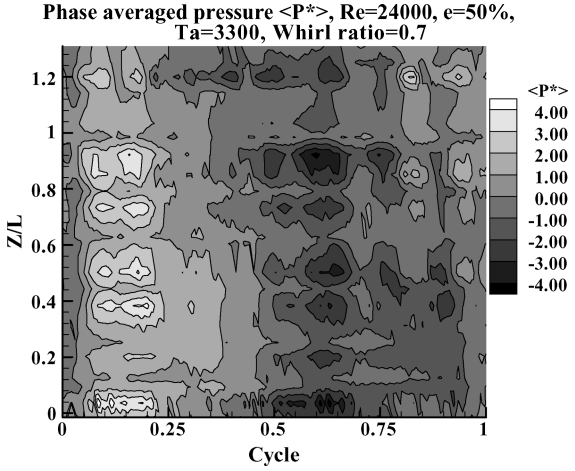

Fig. 14 Phase-averaged pressure contours, whirl ratio = 0.7.

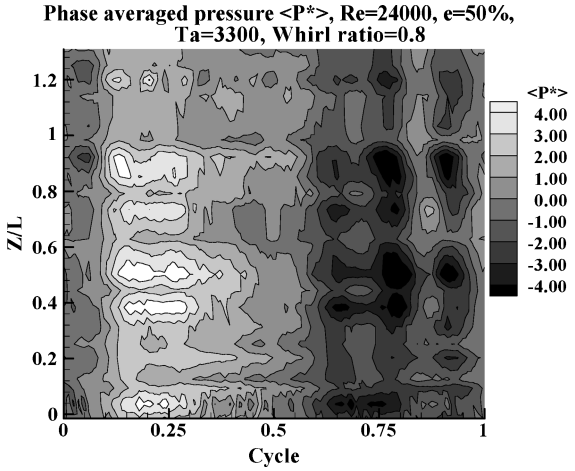

Fig. 15 Phase-averaged pressure contours, whirl ratio = 0.8.

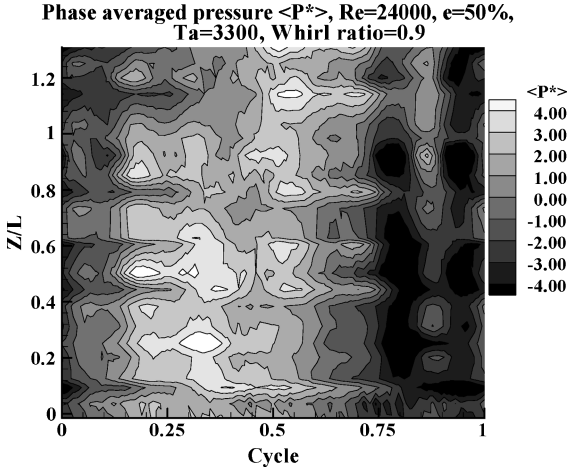

Fig. 16 Phase-averaged pressure contours, whirl ratio = 0.9.

the existence of the high and low pressure regions along the entire length of the seal for the whirling case. The 5% increase in the overall seal pressure drop also implicates the effects of whirling on the flowfield. As the whirl ratio is increased from 0.1 to 0.5, there are slight changes in the distributions with the high-pressure region tending to rotate about 10% of a cycle in the direction of seal rotation from the inlet to the exit, placing the high pressure in the minimum clearance zone.

The whirl ratio 0.6 case represents a departure from these other cases and shows a swapping of the low- and high-pressure regions between the inlet and exit of the seal. Here the high-pressure region has migrated from the pressure side of the seal to the suction side as the flow proceeds toward the seal exit. This also corresponds to the whirl ratio where the seal pressure drop begins to increase. Increasing the whirl ratio to 0.7 appears to greatly shift the phase-averaged pressure distribution with the peak high-pressure region establishing itself at a constant azimuthal location of 0 to 25% of the seal cycle with the low pressures 180 deg opposite at 50 to 75% of the cycle. Between $\omega = 0.6$ and 0.7 a significant increase in the magnitude and coherent organization of the phase-averaged peak

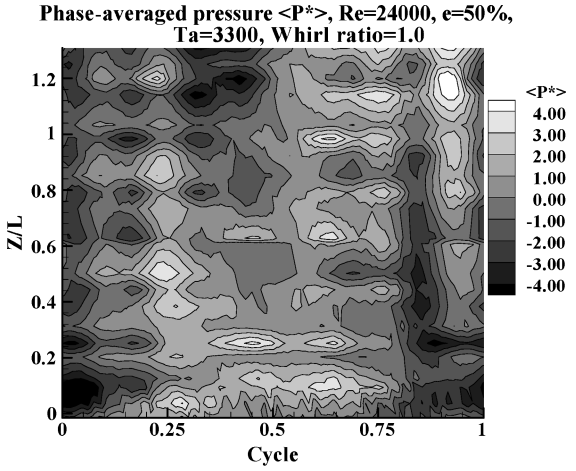

Fig. 17 Phase-averaged pressure contours, whirl ratio = 1.0.

variance is observed. Until now, the separation between the high and low regions was smaller across the minimum clearance (50%). This jump is accompanied by a large increase in the mean pressure drop across the seal. This pressure drop increases to its maximum value as the whirl ratio is increased to 0.8. The magnitude of the phase-averaged pressure variance continues to increase, and it occupies a larger percentage of the seal circumference, almost 50%. The azimuthal locations appear to shift in the direction of seal rotation centered about 25 and 75% of a cycle. Further increases in the whirl ratio continue this shift at 0.9 whirl ratio along with a decrease in pressure variance and the overall mean pressure drop across the seal. At a whirl ratio of 1, the azimuthal variance has become somewhat bimodal with two minimum and maximum pressure locations distributed around the seal. There is a tendency for the positive values to be stronger on the pressure side over the first half of the seal length switching to the suction side over the last half of the seal length. The spread of the high-pressure region increases further and occupies about $\frac{2}{3}$ of the cycle for $\omega = 0.9$ and 1.

The overall trend points to the regions of high and low pressures migrating axially along the seal walls near the exit from the pressure zone to the suction zone between no whirl (static eccentricity) and synchronous whirl condition. The switch in the pressure distribution at the seal exit appears to occur between $\omega = 0.8$ and 0.9, when ΔP decreases after reaching a maximum at $\omega = 0.8$. The shift in the peak pressures is not distinctly seen as noticed by Robic.[4] It is interesting to note that Robic[4] observed the migration to be dependent on the Re/Ta ratio. According to his study, the shift was less pronounced at the Re/Ta ratio under consideration. It can be inferred that the higher axial velocity at $Re = 2.4 \times 10^4$ inhibits the manifestation of the peak pressure migration. This suggests that the Taylor number is very important in the shift, indicating that for a given Reynolds number a higher Taylor number will be necessary for a distinct peak pressure shift. The higher Taylor number was not considered in this study because the required whirl speed of the stator would exceed the capability of the facility. The maximum variation in the magnitude of $\langle P^* \rangle$ for static eccentricity is between ± 7. The peak positive and negative pressures have the highest magnitudes for zero and synchronous whirl. The whirl ratios between 0.1 and 0.6 have pressures fluctuating in the ± 3 range. The whirl ratios from 0.7 to 0.8 display a gradual increase in the magnitude of the peak pressures, reaching a maximum between $\omega = 0.8$ and 1, the range being within ± 7. Characteristically, for all whirls it is observed that the positive pressure zone occupies from 45 to 60% of the stator cycle while the remaining portion is occupied by the suction pressure zone. The maximum positive pressure distribution for the stator cycle occurs typically around the 40% mark for all ω.

For $\omega = 0.7$, discrete axial peak pressure patches emerge at 20 and 65% of the stator cycle between $Z/L = 0$ to 1. This could be the manifestation of Taylor vortices, which caused the axial banding described by Robic[4] and Winslow,[2] except in the present case it is observed at a $Ta = 3300$. The formation of these tiny pressure regions is evident even in $\omega = 0.8$ and 0.9, where the axial striations seem to be breaking up. Lessen[19] indicated the presence of Taylor vortices in the boundary layer of the rotor and stator. Earlier, Schlichting[20] also pointed out the existence of Taylor vortices inside the boundary layer. The differential energy gained by the fluid flowing through the clearance volume caused by the whirling rotor could possibly drive the vortices.

The entrance effect where the flow is subjected to a sudden acceleration into a small annular region is distinctly visible for all whirl ratios between 0.1 to 0.6. The high turbulence at the entrance for these whirls manifests as random pressure fluctuations throughout the cycle up to an axial distance of $Z/L = 0.1$ on the seal surface. A similar effect was evident in the results of Thames[9] and Robic[4] for synchronous whirl ratios. For the higher whirls (0.7 to 1) the entrance region does not show as prominent variations as the lower whirls. This is because of the relative angular velocity between the rotor and stator being lower and the energy imparted by the rotor to the flow at higher whirls not being attenuated. This higher fluid energy subdues the inlet pressure fluctuations seen in the lower whirl ratios. Also, for the higher whirls the rotor imparts more azimuthal momentum to the flow suppressing the external fluctuations caused by the sudden entry. Greater relative velocity between the stator and the rotor for the lower whirl ratios offers a rapidly changing entrance zone to the incoming flow when compared to the higher whirl ratios, causing the instantaneous pressures at the entrance to fluctuate sharply. The disturbance in the pressure distribution noticed near the inlet is not observed at the exit section of the seal.

The static whirl or the zero condition (Fig. 7) has the peak positive pressure around the 150-deg angular location corresponding to 40% of the stator cycle at $Z/L = 0.2$. The high-pressure zone extends up to the end of the seal remaining on the pressure side up to the exit. The lower pressures, as expected, occur in the suction zone where the clearance is increasing. The pressure distribution does not follow Bernoulli's inviscid flow principle according to which a larger clearance would give rise to higher pressures. In our case, the flow is viscous dominated as in a journal bearing and the rotor's viscous drag caused by the eccentric rotor motion creates a pumping effect that transmits higher momentum to the flow, squeezing the fluid into the smaller cross section and increasing the pressure. Between 60 and 65% of the stator cycle, the low pressure extends along the entire axial length of the seal. The higher pressure overlaps about 10% into the suction zone.

A sharp 50% drop in amplitude of peak pressure between zero and 0.1 whirl ratio is noticed. The same pressure range is present up to a $\omega = 0.6$. The overall pressure drop across the seal is relatively constant over this whirl ratio range of 0.1 to 0.6. Contour plots for $\omega = 0.1$ and 0.2 show discrete azimuthal shifts in the maximum pressure locations at $Z/L = 0.4$, 0.7, and $Z/L = 0.2$,0.9 respectively. The lower whirl ratios create smaller azimuthal pressure variances. This can allow the emergence of a flow system resonance. This could also be some type of vortex structure generated by the flow. Normally for a liquid seal, the first resonance frequency is damped out. Between $\omega = 0.1$ to 0.6, the higher pressures remain on the pressure side both at the inlet and the exit. The pressures also remain uniform throughout the cycle along the seal axis with the presence of the occasional patches of high and low pressures. The maximum pressures on the suction and pressure regions start increasing in amplitude between $\omega = 0.7$ and 1. The shift in the exit pressure magnitude begins from $\omega = 0.8$ where the high pressure in the pressure zone at the seal exit is inclining toward the suction zone. It becomes more evident for $\omega = 0.9$ before closely resembling a shift for $\omega = 1$.

Conclusions

This paper explores the effects of the whirl ratio on the mean and transient wall-pressure distributions for a 50% eccentric smooth annular seal. The test section was designed to accommodate fractional whirl ratios. The stator provides the eccentricity settings and rotation independent of the rotor. The tests were performed for $Re = 2.4 \times 10^4$, $Ta = 3300$, and positive whirl ratios as a

continuation of previous work. The overall trend shows that the normalized mean axial pressure distributions are independent of the rotor whirl. The pressure drop across the seal for the different whirl ratios, varied marginally between $\omega = 0.1$ to 0.5, increased for $\omega = 0.6$ to 0.8 and decreased again for $\omega = 0.9$ and 1. The pressure drop for all of the whirling conditions were 5 to 10% larger than for the statically eccentric seal. A 50% drop in the magnitude of the phase-averaged peak pressures occurred when the seal flow condition changed from a static eccentricity to a dynamically whirling seal. As the whirl ratio increases, the azimuthal pressure variation is seen to rise. Dynamic pressures for the statically eccentric condition were almost twice the peak pressures the seal experienced for the smaller whirl ratios. The significant finding of this study was the determination of the whirl ratios at which the peak instantaneous pressures appeared to switch sides from the pressure side to the suction side at the seal exit between an eccentric static seal and a synchronously whirling seal. The switch seemed to occur between $\omega = 0.8$ and 0.9, though the reduction in the amplitude of the peak pressure was noticed between $\omega = 0.1$ to 0.6. The migration in peak pressures was not as distinct as that observed by Robic.[4] It is believed that the high ratio of Reynolds to Taylor number suppressed the clear manifestation of the migration. At $\omega = 0.7$, structures similar to Taylor vortices as reported earlier by Robic[4] were observed. Because of the lower pressures for $\omega = 0.1$ to 0.6, it is believed that running the seal in this whirl range decreases the effect of the seal upon the shaft rotordynamics. Over this range, the pressure variance contours showed only a small amount of change. As the whirl ratio increased from 0.6 to 1, there was a significant amount of shifting in the azimuthal locations of the maximum and minimum pressure as well as an increase in these values. This indicates a varying force (magnitude and direction) being applied to the rotor as the whirl ratio changes. At $\omega = 0.1$ and 0.2, conical projections of high pressures jutting into the "suction zone" are present. These structures are thought to be the disturbances caused to the flow by the system resonance. These are normally subdued by the damping effect of water but showed up in the measurements because of the lower pressures involved in the flow at those whirls. They could also be some type of azimuthal flow vortices created by the rotor viscous drag forces. The pressure data can be used for future simulation and also for rotordynamic analysis.

Acknowledgment

This project was funded by the Turbomachinery Research Consortium at Texas A&M University.

References

[1]Brennen, C., "On the Flow in an Annulus Surrounding a Whirling Cylinder," *Journal of Fluid Mechanics*, Vol. 75, No. 1, 1976, pp. 173–191.

[2]Winslow, R. W., "Dynamic Pressure and Shear Stress Measurements on the Stator Wall of Whirling Annular Seals," M.S. Thesis, Dept. of Mechanical Engineering, Texas A&M Univ., College Station, Dec. 1994.

[3]Morrison, G. L., and Winslow, R. B., "Forces and Moments Generated by Pressure and Shear Stresses on the Stator of a Whirling Eccentric Seal," AIAA Paper 95-2766, 1995.

[4]Robic, B. F., "Experimental and Numerical Analysis of the Effect of Swirl on the Pressure Field in Whirling Annular and Labyrinth Seal," Ph.D. Dissertation, Dept. of Mechanical Engineering, Texas A&M Univ., College Station, May 1999.

[5]Robic, B. F., "Experimental Analysis of the Effect of Swirl on the Pressure Field in Whirling 50% Eccentric Annular Seal," *Proceedings of ASME IGTI TURBO EXPO 2000*, Paper GT-0286, Munich, 2000.

[6]Kaneko, S., "Static and Dynamic Characteristics of Annular Plain Seals," *Third International Conference on Vibration in Machinery*, IMechE, C278, A84, pp. 205–214.

[7]Hashimoto, H., Wada, S., and Sumitomo, M., "The Effects of Fluid Inertia Forces on the Dynamic Behavior of Short Journal Bearings in Super Laminar Flow Regime," *Journal of Tribology*, Vol. 110, July 1988, pp. 539–547.

[8]Johnson, M. C., "Development of a 3-D Laser Doppler Anemometry System: with Measurements in Annular and Labyrinth Seals," Ph.D. Dissertation, Dept. of Mechanical Engineering, Texas A&M Univ., College Station, May 1989.

[9]Thames, H. D., "Mean Flow and Turbulence Characteristics in Whirling Annular Seals," M.S. Thesis, Dept. of Mechanical Engineering, Texas A&M Univ., College Station, May 1992.

[10]Das, P. G., "3-D Laser Doppler Velocimetry Measurements of Eccentric Annular and Labyrinth Seals," M.S. Thesis, Dept. of Mechanical Engineering, Texas A&M Univ., College Station, May 1993.

[11]Shresta, S., "The Effects of Pre-swirl on Flow Through Centered and Eccentric Annular Seals," M.S. Thesis, Dept. of Mechanical Engineering, Texas A&M Univ., College Station, Dec. 1993.

[12]Morrison, G. L., DeOtte, R. E., and Thames, H. D., "Experimental Study of the Flow Field Inside a Whirling Annular Seal," *STLE Tribology Transactions*, Vol. 37, No. 2, 1994, pp. 425–429.

[13]Arghir, M., and Frene, J., "Forces and Moments due to Misalignment Vibration in Annular Liquid Seals Using the Averaged Navier–Stokes Equations," *Journal of Tribology*, Vol. 119, April 1997, pp. 279–290.

[14]Arghir, M., and Frene, J., "Analysis of a Test Case for Annular Seal Flows," *Transactions of the ASME*, Vol. 119, July 1997, pp. 408–414.

[15]Morrison, G. L., Johnson, M. C., and Tatterson, G. B., "Three-Dimensional Laser Anemometer Measurements in an Annular Seal," *Journal of Tribology*, Vol. 113, No. 3, 1991, pp. 421–427.

[16]Morrison, G. L., DeOtte, R. E., and Thames, H. D., "Turbulence Measurements of High Shear Flow Fields in a Turbomachine Seal Configuration," *1992 Conference on Advanced Earth-to-Orbit Propulsion Technology*, Vol. 1, NASA CP-3174, 1992, pp. 457–467.

[17]Olivero-Bally, P., Forestier, B. E., Focquenoy, E., and Olivero, P., "Wall-Pressure Fluctuations in Natural and Manipulated Turbulent Boundary Layers in Air and Water," *Flow Noise Modeling, Measurement, and Control, ASME Winter Annual Meeting*, ASME Publ. FED-Vol. 168, New Orleans, LA, 1993, pp. 63–74.

[18]Nunes, S. J., "A Comparison of Pressure Measurement Systems for an Annular Seal with Whirl," Senior Honor's Thesis, Dept. of Mechanical Engineering, Texas A&M Univ., College Station, Dec. 1993.

[19]Lessen, M., "Turbulent Flow in Shaft Seals and Bearings," *STLE Tribology Transactions*, Vol. 31, No. 3, 1988, pp. 391–396.

[20]Schlichting, H., *Boundary Layer Theory*, McGraw–Hill, New York, 1979.